

MICROCOPY RESOLUTION TEST CHART NATIONAL BUREAU OF STANDARDS-1963-A



NAVAL POSTGRADUATE SCHOOL

Monterey, California





THESIS

MEASUREMENT OF PUMPED SUPERLUMINAL ELECTROMAGNETIC RADIATION

bу

William More Decker, IV and Joseph Paul Mackin

June 1980

Thesis Advisor:

F. R. Buskirk

Approved for public release; distribution unlimited.

ODE FILE COPY

80 12 01 047

SECURITY CLASSIFICATION OF THIS PAGE (Then Date Entered)

AD-AC92306 ITLE (and Submitte) Measurement of Pumped Superluminal Electromagnetic Radiation. Master's Thesis June 1980 Enforming Organization name and address Naval Postgraduate School Monterey, California 93940 Entropy C		PAGE READ INSTRUCTIONS BEFORE COMPLETING FORM
Measurement of Pumped Superluminal Electromagnetic Radiation. Jume 1980 PERFORMING ORGANIZATION NAME AND ADDRESS Naval Postgraduate School Monterey, California 93940 CONTROLLING OFFICE NAME AND ADDRESS Naval Postgraduate School Monterey, California 93940 CONTROLLING OFFICE NAME AND ADDRESS Naval Postgraduate School Monterey, California 93940 CONTROLLING OFFICE NAME AND ADDRESS Naval Postgraduate School Monterey, California 93940 CONTROLLING OFFICE NAME AND ADDRESS NAVAL POSTGRADUATE SCHOOL MONTEREY, California 93940 CONTROLLING OFFICE NAME AND ADDRESS NAVAL POSTGRADUATE SCHOOL MONTEREY, California 93940 CONTROLLING OFFICE NAME AND ADDRESS NAVAL POSTGRADUATE SCHOOL MONTEREY, California 93940 CONTROLLING OFFICE NAME AND ADDRESS NAVAL POSTGRADUATE SCHOOL MONTEREY, California 93940 CONTROLLING OFFICE NAME AND ADDRESS NAVAL POSTGRADUATE SCHOOL MONTEREY, CALIFORNIA OFFICE NAME AND ADDRESS OFFI MUMBER OF PAGES OFFI MUMBER OFFI MUMB		2. GOVT ACCESSION NO. 1. RECIPIENT'S CATALOG NUMBER
Measurement of Pumped Superluminal Electromagnetic Radiation, Waster's Thesis June 1980 Free Promise one Report Number William More / Decker, IV Joseph Paul / Mackin Enforming oncamization wame and address Naval Postgraduate School Monterey, California 93940 CONTROLLING OFFICE NAME AND ADDRESS Naval Postgraduate School Monterey, California 93940 CONTROLLING OFFICE NAME AND ADDRESS Naval Postgraduate School Monterey, California 93940 CONTROLLING OFFICE NAME AND ADDRESS Naval Postgraduate School Monterey, California 93940 CONTROLLING OFFICE NAME AND ADDRESS Naval Postgraduate School Monterey, California 93940 CONTROLLING OFFICE NAME AND ADDRESS Naval Postgraduate School Monterey, California 93940 The Report Date June 1980 The Report		
Electromagnetic Radiation . Dura 1980 Duranted and and address and address Naval Postgraduate School Monterey, California 93940 Contracting office was and address Naval Postgraduate School Monterey, California 93940 Contracting office was and address Naval Postgraduate School Monterey, California 93940 Contracting office was and address Naval Postgraduate School Monterey, California 93940 Contracting office was and address Duranted School Monterey, California 93940 Contracting office was seen and address Duranted School Monterey of Page 65 June 1980 19. Report Date June 1980 19. Magnetic Office of Magnetic Militerant from Controlling Office) In SECURITY CLASS. (of this report) Unclassified The Decination of Page 65 Internation Statement (of this Report) Approved for public release; distribution unlimited.	- · · · · · · · · · · · · · · · · · · ·	, , , , , , , , , , , , , , , , , , , ,
UTHOR/s, William More /Decker, IV Joseph Paul Mackin ERFORMING ORGANIZATION NAME AND ADDRESS Naval Postgraduate School Monterey, California 93940 EDITORILING OFFICE NAME AND ADDRESS Naval Postgraduate School Monterey, California 93940 EDITORILING OFFICE NAME AND ADDRESS Naval Postgraduate School Monterey, California 93940 EDITORILING AGENCY NAME & ADDRESS/II different from Controlling Office) IS. SECURITY CLASS. (of this report) Unclassified IS. DECURITY CLASS. (of this report) Approved for public release; distribution unlimited. ISTRIBUTION STATEMENT (of the shortest entered in Block 29, II different from Report) Magnetic Undulator Cerenkov Radiation		
William More/Decker, IV Joseph Paul Mackin EMPONNING ORGANIZATION NAME AND ADDRESS Naval Postgraduate School Monterey, California 93940 CONTROLLING OFFICE NAME AND ADDRESS Naval Postgraduate School Monterey, California 93940 CONTROLLING OFFICE NAME AND ADDRESS Naval Postgraduate School Monterey, California 93940 CONTROLLING OFFICE NAME AND ADDRESS Naval Postgraduate School Monterey, California 93940 IS REPORT DATE June 1980 13. REPORT DATE June 1980 14. REPORT DATE June 1980 15. REPORT DATE June 1980 15. REPORT DATE June 1980 15. REPORT DATE	rectromagnetic Radiation,	6. PERFORMING ORG. REPORT NUMBE
William More/Decker, IV Joseph Paul Mackin EMPONNING ORGANIZATION NAME AND ADDRESS Naval Postgraduate School Monterey, California 93940 CONTROLLING OFFICE NAME AND ADDRESS Naval Postgraduate School Monterey, California 93940 CONTROLLING OFFICE NAME AND ADDRESS Naval Postgraduate School Monterey, California 93940 CONTROLLING OFFICE NAME AND ADDRESS Naval Postgraduate School Monterey, California 93940 IS REPORT DATE June 1980 13. REPORT DATE June 1980 14. REPORT DATE June 1980 15. REPORT DATE June 1980 15. REPORT DATE June 1980 15. REPORT DATE	• • •	
Joseph Paul Mackin Enforming Ordanization name and address Naval Postgraduate School Monterey, California 93940 CONTROLLING OFFICE NAME AND ADDRESS Naval Postgraduate School Monterey, California 93940 CONTROLLING OFFICE NAME AND ADDRESS Naval Postgraduate School Monterey, California 93940 SCHITORING AGENCY NAME & ADDRESS(II different from Controlling Office) William 1980 13. NEPORT DATE June 1980 14. NEPORT DATE June 1980 15. NECURITY CLASS. (of this report) Unclassified The DECLASSIFICATION/DOWNGRAM SCHEOULE THE DECLASSIFICATION/DOWNGRAM SCHEOULE		S. CONTRACT OR GRANT NUMBER(s)
EMPORMING ORGANIZATION NAME AND ADDRESS Naval Postgraduate School Monterey, California 93940 ENTROLLING OFFICE NAME AND ADDRESS Naval Postgraduate School Monterey, California 93940 ENTROLLING OFFICE NAME ADDRESS Naval Postgraduate School Monterey, California 93940 ENTROPH DATE June 1980 19. NUMBER OF PAGES 65 10. SECURITY CLASS. (of this report) Unclassified The DECLASSIFICATION/DOWNGRAM SCHEDULE TATEMENT (of this Report) Approved for public release; distribution unlimited.		
Naval Postgraduate School Monterey, California 93940 CONTROLLING OFFICE NAME AND ADDRESS Naval Postgraduate School Monterey, California 93940 Monterey, California 93940 IS REPORT DATE June 1980 19. NUMBER OF PAGES 65 IS SECURITY CLASS. (of this report) Unclassified IS DECLASSIFICATION/DOWNGRAM SCHEDULE ISTRIBUTION STATEMENT (of this Report) Approved for public release; distribution unlimited. ISTRIBUTION STATEMENT (of the electron entered in Stock 30. If different from Report) UPPLEMENTARY NOTES EY WORDS (Continue on reverse side if necessary and identify by block number) Magnetic Undulator Cerenkov Radiation	- Coopii Taaajiiaoiiii	
Monterey, California 93940 CONTROLLING OFFICE NAME AND ADDRESS Naval Postgraduate School Monterey, California 93940 Monterey, California 93940 IS. REPORT DATE June 1980 19. NUMBER OF PAGES 65 IONITORING AGENCY NAME & ADDRESS(II different from Controlling Office) Unclassified The DECLASSIFICATION/DOWNGRAM SCHEOULE ISTRIBUTION STATEMENT (of this Report) Approved for public release; distribution unlimited. ISTRIBUTION STATEMENT (of this charrent entered in Block 26, 11 different from Report) UPPLEMENTARY NOTES EV WORDS (Continue on reverse side if necessary and identify by block number) Magnetic Undulator Cerenkov Radiation		10. PROGRAM ELEMENT, PROJECT, TA
Naval Postgraduate School Monterey, California 93940 19. Numer 1980 19. Numer of Pages 65 IONITORING AGENCY NAME & ADDRESS(II different from Controlling Office) Unclassified 18. SECURITY CLASS (of this report) Unclassified 18. DECLASSIFICATION/Downgrad SCHEDULE 18. TREPORT DATE 5. SECURITY CLASS (of this report) Unclassified 18. DECLASSIFICATION/Downgrad 18. SECURITY CLASS (of this report) Unclassified 18. DECLASSIFICATION/Downgrad 18. SECURITY CLASS (of this report) Unclassified 18. DECLASSIFICATION/Downgrad 18. SECURITY CLASS (of this report) Unclassified 18. DECLASSIFICATION/Downgrad 18. SECURITY CLASS (of this report) Unclassified 18. DECLASSIFICATION/Downgrad 18. SECURITY CLASS (of this report) Unclassified 18. DECLASSIFICATION/Downgrad 18. SECURITY CLASS (of this report) Unclassified 18. DECLASSIFICATION/Downgrad 18. SECURITY CLASS (of this report) Unclassified 18. DECLASSIFICATION/Downgrad 18. SECURITY CLASS (of this report) Unclassified 18. DECLASSIFICATION/Downgrad 18. SECURITY CLASS (of this report) Unclassified 18. DECLASSIFICATION/Downgrad 18. DEC		
Naval Postgraduate School Monterey, California 93940 13. NUMBER OF PAGES 65 16. SECURITY CLASS. (of this report) Unclassified 18. DECLASSIFICATION/DOWNGRAM STRIBUTION STATEMENT (of this Report) Approved for public release; distribution unlimited. 15. TRIBUTION STATEMENT (of the charrons entered in Block 26, if different from Report) UPPLEMENTARY NOTES EY WORDS (Continue on reverse side if necessary and identify by block number) Magnetic Undulator Cerenkov Radiation	Monterey, California 93940	
Naval Postgraduate School Monterey, California 93940 13. NUMBER OF PAGES 65 16. SECURITY CLASS. (of this report) Unclassified 18. DECLASSIFICATION/DOWNGRAM STRIBUTION STATEMENT (of this Report) Approved for public release; distribution unlimited. 15. TRIBUTION STATEMENT (of the charrons entered in Block 26, if different from Report) UPPLEMENTARY NOTES EY WORDS (Continue on reverse side if necessary and identify by block number) Magnetic Undulator Cerenkov Radiation	TROLLING OFFICE NAME AND ADDRESS	VIZ. REPORT DATE
Monterey, California 93940 19. Number of Pages 65 1001170RING AGENCY NAME & AGDRESS(1) different from Controlling Office) Unclassified 18. DECLASSIFICATION/DOWNGRAM SCHEDULE 18. TRIBUTION STATEMENT (of this Report) Approved for public release; distribution unlimited. 18. SECURITY CLASS. (of this report) Unclassified 18. DECLASSIFICATION/DOWNGRAM SCHEDULE	- -	\sim 7.4 M
Unclassified The DECL ASSIFICATION/DOWNGRAM RESTRIBUTION STATEMENT (of this Report) Approved for public release; distribution unlimited. ISTRIBUTION STATEMENT (of the shormer entered in Block 20, if different from Report) Unclassified The DECL ASSIFICATION/DOWNGRAM SCHEDULE RESTRIBUTION STATEMENT (of the shormer entered in Block 20, if different from Report) UPPLEMENTARY NOTES EV WORDS (Continue on reverse side if necessary and identity by block number) Magnetic Undulator Cerenkov Radiation		13. NUMBER OF PAGES
Unclassified 18a. DECLASSIFICATION/DOWNGRAM SCHEDULE RESTRIBUTION STATEMENT (of this Report) Approved for public release; distribution unlimited. ISTRIBUTION STATEMENT (of the shortest entered in Block 26, if different from Report) UPPLEMENTARY NOTES EV WORDS (Continue on reverse side if necessary and identify by block member) Magnetic Undulator Cerenkov Radiation	TOBING AGENCY NAME & ADDRESS/I different	
Approved for public release; distribution unlimited. ISTRIBUTION STATEMENT (of the shorrest entered in Block 20, if different from Report) UPPLEMENTARY NOTES EY WORDS (Continue on reverse side if necessary and identify by block number) Magnetic Undulator Cerenkov Radiation		
Approved for public release; distribution unlimited. ISTRIBUTION STATEMENT (of the chargest entered in Block 20, if different from Report) LEY WORDS (Continue on reverse side if necessary and identify by block number) Magnetic Undulator Cerenkov Radiation		onciassified
Approved for public release; distribution unlimited. ISTRIBUTION STATEMENT (of the chargest entered in Block 20, II different from Report) UPPLEMENTARY NOTES Ev WORDS (Continue on reverse side II necessary and identify by block number) Magnetic Undulator Cerenkov Radiation		184. DECLASSIFICATION/DOWNGRADII
EV WORDS (Continue on revote side if necessary and identify by block number) Magnetic Undulator Cerenkov Radiation	AND THE STATE OF T	
EV WORDS (Continue on revoces side if necessary and identify by block number) Magnetic Undulator Cerenkov Radiation	Approved for public releas	e; distribution unlimited.
Ev words (Continue on review side if necessary and identify by block number) Magnetic Undulator Cerenkov Radiation	Approved for public releas	e; distribution unlimited.
Magnetic Undulator Cerenkov Radiation	<u> </u>	
Magnetic Undulator Cerenkov Radiation	RIBUTION STATEMENT (of the charges entered in	
Magnetic Undulator Cerenkov Radiation	RIBUTION STATEMENT (of the charges entered in	
Cerenkov Radiation	. RIBUTION STATEMENT fol the sherrest entered is	n Block 30, II different from Report)
	RIBUTION STATEMENT (of the shortest entered in PLEMENTARY NOTES FORDS (Continue on reverse side if necessary and	n Block 30, II different from Report)
	RIBUTION STATEMENT (of the chargest entered in PLEMENTARY NOTES FORDS (Constitute on review aldo if necessory and lagnetic Undulator	n Block 30, II different from Report)
	RIBUTION STATEMENT (of the charges entered in the charge entered entered in the charge entered entered in the charge entered ent	n Block 30, II different from Report)
ATT BACT (Continue on control of the II personner and (death) by black combat	RIBUTION STATEMENT (of the charges entered in the charge entered entered in the charge entered entered in the charge entered ent	n Block 30, II different from Report)
A new source of radiation has been postulated that occurs	ECRES (Continue on reverse side if necessary and lagnetic Undulator errors Radiation Superluminal	n Block 26, II different from Report) I identify by block member)
hen a charged particle, moving with a velocity greater than	PLEMENTARY NOTES WORDS (Continue on reverse side if necessary and lagnetic Undulator errenkov Radiation Superluminal	n Block 26, il different from Report) i identify by block member)
he velocity of light in a medium, is caused to oscillate abou	ECT (Continuo en reverse alde II necessary and A new source of radiation	identify by bleek number) Identify by bleek number) Identify by bleek number)
ts transverse beam line by means of a static, periodic magnet	PLEMENTARY NOTES WORDS (Continue on reverse side if necessary and lagnetic Undulator Gerenkov Radiation Guperluminal RACT (Continue on reverse side if necessary and a new source of radiation in a charged particle, moving velocity of light in a me	Identify by block number) I dentify by block number) In has been postulated that occurs ing with a velocity greater than edium, is caused to oscillate about
r electric field or by means of an incident transverse wave.	PLEMENTARY NOTES WORDS (Continue on revoce side if necessary and lagnetic Undulator Gerenkov Radiation Guperluminal RACT (Continue on revoce side if necessary and a new source of radiation in a charged particle, moving velocity of light in a metransverse beam line by metransverse beam line by metransverse beam line by metransverse side in the second side in second side in the second side	identify by block number) Identify by block number) In has been postulated that occurs ing with a velocity greater than edium, is caused to oscillate about means of a static, periodic magnetic
xperiments were conducted to measure this new source of elec- romagnetic shock radiation. and compare it to Cerenkov radiat	ECRES (Continue on revoce side if necessary and lagnetic Undulator superluminal RACT (Continue on revoce and if necessary and a new source of radiation in a charged particle, moving velocity of light in a metansverse beam line by means electric field or by means	Identify by Neck manber) Identify by Neck manber) In has been postulated that occurs ing with a velocity greater than edium, is caused to oscillate about means of a static, periodic magnetics of an incident transverse wave.

DD 1 JAN 73 1473 (Page 1)

EDITION OF 1 WOV 68 IS OBSOLETE S/N 0102-014-4601 :

UNCLASSIFIED OF THIS PAGE (Then Date Shiered)

(20. ABSTRACT Continued)

a known source of electromagnetic shock radiation. The preliminary results agree with predictions of Schneider and Spitzer, but the present accuracy is not sufficient to rule out alternative theories.

Access	ion For	
NTIS		X
DDC TA		Ц
Unanno		. 🗀
Justif	ication	1
Ву		
Pistri	bution	/
finil	ुः	Codes
	Availa	and/or
Dist	speci	al
Н		i
		1

Approved for public release; distribution unlimited

Measurement of Pumped Superluminal Electromagnetic Radiation

ру

William More Decker, IV Captain, United States Army B.S., Cornell University, 1970

and

Joseph Paul Mackin
Captain, United States Army
B.S., United States Military Academy, 1974

Submitted in partial fulfillment of the requirements for the degree of

MASTER OF SCIENCE IN PHYSICS

from the

NAVAL POSTGRADUATE SCHOOL June 1980

Authors:	(-je & 50
	Jest Mork
Approved by:	Fred R Bushing
	Thesis Advisor
	Mayer
	Second Reader
	Chairman, Department of Physics and Chemistry
	Chairman, Department of Physics and Chemistry
	William M. Tolles
	Dean of Science and Engineering

ABSTRACT

A new source of radiation has been postulated that occurs when a charged particle, moving with a velocity greater than the velocity of light in a medium, is caused to oscillate about its transverse beam line by means of a static, periodic magnetic or electric field or by means of an incident transverse wave. Experiments were conducted to measure this new source of electromagnetic shock radiation, and compare it to Cerenkov radiation, a known source of electromagnetic shock radiation. The preliminary results agree with predictions of Schneider and Spitzer, but the present accuracy is not sufficient to rule out alternative theories.

TABLE OF CONTENTS

I.	INTRODU	JCTION	9
II.	THEORY	***************************************	11
III.	MAGNET	CC UNDULATOR	19
.VI	EXPERIM	MENTAL PROCEDURE	36
٧.	ANALYS	[S	42
APPENI	X A:	BEAM SPREAD	47
APPENI	DIX B:	PSER THRESHOLD	51
APPENI	OIX C:	TRAVELING MAGNETIC FIELD FLUXMETER	54
APPENI	OIX D:	OPTICS	56
LIST (F REFER	RENCES	64
INITIA	L DISTE	RIBUTION LIST	65

LIST OF TABLES

1.	Comparison of magnet configurations	23
2.	Angular deviation due to scatterers	37
3.	Cerenkov angle of air and helium	37
4.	Summary of results, run # 1	40
5•	Summary of results, run # 2	40
6.	Summary of results, run # 3	41

LIST OF FIGURES

1.	Mach Cone	18
2.	Ellis Magnet	21
3.	First "C" Magnet	25
4.	Permanent Magnet	27
5.	Prototype Comb Magnet	27
6.	Magnetic Field of Prototype at 8.0A and with a 9.0cm Period	28
7.	Magnetic Field of Prototype at 12.0A and with a 10.2cm Period	29
8.	Magnetic Field of Prototype at 16.0A and with a 10.2cm Period	-
9.	Final Magnetic Undulator	32
10.	Magnetic Field of Final Magnet at 8.0A and with a 9.0cm Period	33
11.	Magnetic Field of Final Magnet at 10.0A and with a 7.0cm Period	34
12.	Radiation Pattern for Cerenkov Radiation	44
13.	Radiation Pattern for PSER Radiation	44
14.	Graph of Cerenkov Angle vs. Scattering Angle of Exit Window	50
15.	Traveling Fluxmeter	55
16.	Initial Optical Configuration	58
17.	Second Optical Configuration	59
18.	Photodiode Installed in Camera	60
19.	Schematic of Photodiode Circuit	61
20.	Final Configuration	62

<u>ACKNOWLEDGEMENTS</u>

We would like to thank Professor F.R. Buskirk for his many hours of patient guidance throughout our endeavor. Without his advice and knowledge, we would have accomplished virtually nothing.

We would like to thank Mr. H. McFarland and Mr. D. Snyder, whose many innovative ideas greatly assisted us towards our goal.

We would like to thank Lt. Jerry Graham for being our partner during this work, and to wish him great success in the culmination of this project.

Last, but by no means least, we would like to thank our wives and families for their kind and loving support during the conduct of this work.

I. <u>INTRODUCTION</u>

It is a well-known phenomenon that when an electron moves through a medium with a velocity that exceeds the speed of light in that medium, Cerenkov radiation will be produced [Ref. 1]. It has been proposed by S. Schneider and R. Spitzer that when such an electron is given an oscillatory motion transverse to its beam line, a new form of electromagnetic radiation will be produced [Ref. 2]. Such a transverse oscillation may be superimposed by means of a static, transverse, spatially periodic electric or magnetic field, or by means of an incident transverse electromagnetic This form of radiation was described initially by Schneider and Spitzer as stimulated electromagnetic shock radiation (SESR), but due to controversy over the use of the word stimulated, this terminology was dropped [Ref. 3]. In this paper, the term pumped superluminal electromagnetic radiation (PSER) will be used.

This work was undertaken to measure the intensity of PSER vis-a-vis Cerenkov radiation. The effort was conducted in two phases; the choice and construction of a suitable pump field, and the measurement of the PSER and Cerenkov radiation. The choice of a suitable pump field was a continuation of the work begun by Ellis [Ref. 4]. A transverse periodic magnetic field, henceforth called an undulator, was chosen for reasons specified in Chapter III.

The measurement of the intensities of the Cerenkov radiation and PSER involved the modification of the Naval Postgraduate School Linear Accelerator (LINAC). A variety of different schemes were tried, as outlined in Chapter IV. The results of the experiments are compared in Chapter V.

II. THEORY

When a charged particle moves through a medium with a velocity that is greater than the velocity of light in that medium, electromagnetic radiation is produced which is similar in nature to an acoustical shock wave [Ref. 1]. This radiation is called Cerenkov, after its discoverer, and is a form of electromagnetic shock radiation.

It is now proposed by Schneider and Spitzer that there is another form of electromagnetic shock radiation that can be produced by the oscillatory motion of an electron transverse to its beam line in a medium where its velocity exceeds that of light in that medium. This radiation, pumped superluminal electromagnetic radiation (PSER), is distinct from Cerenkov radiation. N. Kroll has disputed this claim of a new form of radiation, and asserts that it is simply the emission of Cerenkov radiation about the particle's instantaneous direction of motion [Ref. 5]. This outline attempts to give a general understanding of the differences between PSER and Cerenkov radiation as proposed by Schneider and Spitzer.

In the theory proposed by Schneider and Spitzer, the PSER is described as a new effect that comprises the production of coherent electromagnetic waves in a polarizable medium. Coherent, as defined by Schneider and Spitzer in

Ref. 2, means that radiation from the polarization currents induced at different points along the trajectory of the electron adds in phase in a specific direction. In the original proposal [Ref. 2], the PSER was proposed as a narrowband, intense, tunable source of electromagnetic radiation. Later revisions now propose a broadband effect [Ref. 3]. The theory is applicable to a dispersionless medium, and is restricted to a linear response, i.e. where the dielectric constant is equal to the square of the index of refraction, and is in fact constant. The theory is essentially classical, and involves only the Maxwell and Lorentz equations in a polarizable medium and the Lorentz force.

PSER can be thought of as the synergistic interaction of radiation which is Doppler-shifted in frequency by Compton backscattering in vacuum from relativistic charged particles and the production of a shock wave which occurs when a relativistic particle exceeds the speed of light in a medium. When a charged particle is accelerated in a vacuum by an electromagnetic wave, the frequency of the radiated wave is upshifted with respect to the incident wave, so that the frequency of the emitted wave is

 $\omega = \gamma^2 \, (1-\cos\,\theta)(1+\cos\,\theta') \, \omega_o$. (II-1) γ is the kinetic energy of the beam divided by the rest energy of the charged particle, ω_o is the frequency of the incident wave, θ is the collision angle, and θ' is the scattering angle. For the case of the static, periodic

field, the cos θ term is dropped, and ω_o is defined [Ref. 6], $\omega_o = 2\pi c/\lambda_o \qquad \qquad (II-2)$

where λ_{\circ} is the spatial period of the static field. In either the static field or traveling wave case, the energy to produce the frequency upshift is provided by the moving charged particle.

An electromagnetic shock wave is produced when a charged particle exceeds the speed of light in a medium. The interaction of the Coulomb field of the charged particle with the medium produces transverse electromagnetic waves. Due to the particle's superluminal condition (speed in excess of light in the medium), the effect has a collective response from the medium, not individual responses from the separate atoms. It is the simultaneous occurence of the shock radiation with the Doppler-shift of the scattered radiation that produces PSER. In this thesis work, the focus was to measure the intensity of PSER relative to that of Cerenkov radiation. The subsequent discussion focuses on the difference between the two forms of radiation.

The mechanism for both Cerenkov radiation and PSER is the response of the medium to the Coulomb field of the incident electron transformed to the rest frame of the medium. The different effects are due to the difference in the field of the oscillating electron vis-a-vis the field of the non-oscillating electron. In both cases, the beam is a source of an electromagnetic field which induces polarization

charges and currents in the medium. The incident beam has a charge and current distribution. These distributions dictate the electric and magnetic fields of the beam. The latter fields induce in the medium a charge and current distribution. It is this induced distribution that is the source of the emitted electric and magnetic fields. In terms of Maxwell's equations (cgs units),

$$\nabla \cdot \overline{B} = 0 \tag{II-3}$$

$$\nabla \cdot \mathbf{\bar{E}} = 4\pi \rho_{\text{total}} \tag{II-4}$$

$$\nabla \mathbf{x} \mathbf{\overline{E}} + \partial \mathbf{\overline{B}}/\partial ct = 0$$
 (II-5)

$$\nabla \mathbf{\bar{x}} \mathbf{\bar{B}} + \partial \mathbf{\bar{E}}/\partial ct = (4\pi/c) \mathbf{\bar{j}}_{total}$$
 (II-6)

$$\rho_{\text{total}} = \rho_{\text{beam}} + \rho_{\text{induced}}$$
 (II-7)

$$\overline{j}_{total} = \overline{j}_{beam} + \overline{j}_{induced}$$
 (II-8)

The contribution to the field due to the induced sources is represented by the polarization vector, \overline{P} , where

$$\rho_{\text{induced}} = \sqrt{\overline{P}}$$
(II-9)

and

$$\overline{j}_{induced} = \partial \overline{P}/\partial t$$
. (II-10)

The field \overline{P} is related to the \overline{E} field produced by the induced sources by the displacement vector, \overline{D} , where

$$\overline{D} = \overline{E} + 4\pi \overline{P}. \qquad (II-11)$$

Maxwell's equations then become

$$\nabla \cdot \overline{D} = 4\pi \rho_{\text{beam}}$$
 (II-12)

and

$$\sqrt{x} \times B - \partial D/\partial ct = (4\pi/c) \overline{J}_{beam}$$
 (II-13)

In a linear medium, \overline{D} is related to \overline{E} by

$$\overline{D} = \epsilon \overline{E} \tag{II-14}$$

where \in is the dielectric constant of the medium.

The solutions of these equations yield the radiated electric and magnetic fields. The difference between the Cerenkov radiation and the PSER is in the applicable density function and current function arising from the oscillatory motion of the electron. The Cerenkov radiation involves the response of the medium to the charge density and the purely convective current, which is independent of the incident electromagnetic wave or the superimposed static, periodic magnetic field. The PSER is due to the current produced by the oscillatory motion of the electron.

Schneider and Spitzer [Ref. 3] predict that the PSER radiation will have two components; a longitudinal component and a transverse component. The longitudinal component is approximately the same as the Cerenkov radiation, and in energy per unit path length is

$$\frac{dW}{dz_{T}} \cong \frac{dW}{dz_{C}} = \frac{e^{2}}{c^{2}} \int \omega d\omega (1-1/\beta^{2} \epsilon). (II-15)$$

 β is the drift velocity divided by the speed of light. The limits of integration are from zero to the resonance frequency, ω_{r} . The transverse component is

$$\frac{dW}{dz_{T}} = \frac{e^{2}(\omega_{T}\omega_{1}/\Omega\omega_{0})^{5/3}}{u^{2}(\overline{\beta}_{z}^{2}(-1)^{1/6}\gamma^{5/3})} (.74)\Omega^{2} . (II-16)$$

where

 ω_{r} resonance frequency of medium

ω₁ Lamor frequency = eB_{e/mc}

Bo maximum magnetic field

u drift velocity

 $\overline{\beta}_z$ average drift velocity divided by speed

of light, and

$$\Omega = \beta n \omega_0 = 2\pi c \beta / L$$

where L is the spatial period of the pump field. The average drift speed accounts for the energy going into the radial component of velocity of the electron. Since the longitudinal component is approximately the same as the Cerenkov radiation, the increase in intensity is

$$\frac{dW_{T}}{dW_{C}} = \text{intensity increase.}$$
 (II-17)

It is this value that this work attempted to measure.

There are other differences in the two forms of radiation produced. Schneider and Spitzer [Ref. 3] predict that PSER will have two radiation bands as compared to one for Cerenkov radiation. The lower band has threshold at

$$\omega_{+} = \Omega_{S}(\beta n - 1) \tag{II-18}$$

and the higher band at

$$\omega_{-} = \Omega_{s}(\beta n+1). \qquad (II-19)$$

The quantity $\Omega_{\mathbf{S}}$ is a dynamically derived quantity and is

$$\Omega_{s} = \Omega/(\beta^{2} \epsilon_{o} - 1). \tag{II-19}$$

Although the authors state that this result cannot be derived kinematically, it is of interest to note that the

same value can be arrived at kinematically, although the angular distribution is different. This is outlined in Appendix B.

Another possible point of experimental verification may be in the Mach cone distibution. The Mach angle for the Cerenkov radiation is given [Ref. 2]

$$\sin \dot{\phi}_{c} = (\beta^{2} \epsilon)^{-1}. \tag{II-20}$$

The value ∈ is taken as a constant for the dispersionless medium considered. For PSER, however, in Ref. 3, the Mach angle is given as

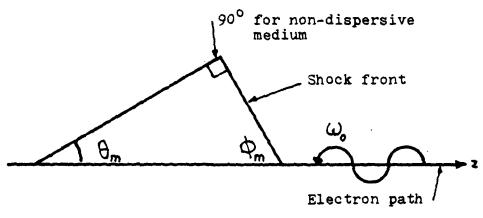
$$\sin \mathcal{D}_{M} = \left[\beta \in (\omega_{M})^{\frac{1}{2}}\right]^{-1}. \tag{II-21}$$

The two values of ϵ will be different, but the difference may be very slight. The value of ϵ for the Cerenkov case is taken at the mean value in the visible region. The value for $\epsilon(\alpha_{\mathbf{M}})$ is taken where

$$\alpha_{\mathrm{M}} = \left[\epsilon_{\mathrm{o}} (\beta^{2} \epsilon_{\mathrm{o}} - 1) / 3(\epsilon_{\mathrm{o}} - 1) \right]^{\frac{1}{4}} \left(\Omega_{\mathrm{g}} \alpha_{\mathrm{r}} \right)^{\frac{1}{2}} \left(\mathrm{II} - 22 \right)$$

The value of ϵ_{\bullet} is ϵ evaluated at x_{\bullet} .

For the dispersionless case, the complementary angle of the Mach angle is the photon emission angle, $\theta_{_{\hbox{\scriptsize C}}}$ for the Cerenkov radiation, and $\theta_{_{\hbox{\scriptsize M}}}$ for PSER. This is shown in figure 1.



MACH CONE

FIGURE 1

III. MAGNETIC UNDULATOR

In order to generate PSER, the electron beam must interact with a static periodic transverse electric field, a static periodic transverse magnetic field or an electromagnetic wave propagating into the electron beam. A modest static periodic magnetic field (200 gauss) affects the electrons as much as very high powered (100 megawatt) electromagnetic waves or high electric fields (6.1 megavolts/meter). The three equivalent pump regimes are developed below.

$$\overline{S} = \overline{E} \times \overline{H}$$

$$S = \frac{E B}{\mu_0}, \text{ and for a plane wave } \frac{E}{B} = c$$

$$S = \frac{c B^2}{\mu_0}, \text{ or } S = \frac{E^2}{\mu_0}$$

For a 100 megawatt electromagnetic wave propagating in a cylindrical cavity of diameter = $3.6 \text{ cm} (0.001 \text{ m}^2 \text{ crosssectional})$ area) the Poynting vector is,

$$S = \frac{1 \times 10^8 \text{ watts}}{0.001 \text{ m}^2} = 10^{11} \text{ watts/m}^2.$$

An equivalent static periodic electric field is

$$E^2 = \mu_0 cs = 4\pi \times 10^{-7} \text{ H/m} \times 3 \times 10^8 \text{ m/s} \times 10^{11} \text{ w/m}^2$$

or
$$E = 6.14 \times 10^6 \text{ volts/meter}$$
.

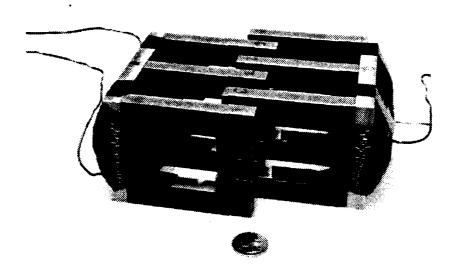
An equivalent static periodic magnetic field is

$$B^{2} = \frac{S\mu_{0}}{c} = \frac{10^{11} \text{ w/m}^{2} \text{ x } 4\pi \text{ x } 10^{-7} \text{ H/m}}{3 \text{ x } 10^{8} \text{ m/s}}$$

$$B = 2.05 \text{ x } 10^{-2} \text{ Tesla} = 205 \text{ gauss}.$$

These calculations were the basis for the decision to pump the electrons with a magnetic undulator. Based upon the theoretical analysis of Schneider and Spitzer [Ref. 3] an undulator with a minimum field of 100 gauss and a period between 5.0 cm and 10.0 cm was needed if the PSER was to be of significant magnitude with respect to the Cerenkov radiation. The undulator was determined to need a gap of 2.0 cm between the pole tips to allow the Cerenkov and PSER cones to be unobstructed (see Appendix A). The field needed to be as close to sinusoidal as possible in order to avoid higher order Fourier components. As the electron beam was 1.9 cm in diameter at the final magnet, linearity over at least 1.5 cm in the vertical direction was highly desireable. To determine if a particular magnetic undulator prototype met these criteria, a traveling magnetic field fluxmeter was constructed and the output recorded on an X - Y plotter (see Appendix C).

The starting point for the construction of the spatially periodic transverse magnetic field was the configuration developed by Ellis (Figure 2)[Ref. 4]. A study of the design of this magnetic undulator disclosed several limitations. The Ellis undulator was unable to dissipate the heat generated by the high currents needed to establish magnetic fields of approximately one kilogauss. The pole tip design was such



ELLIS MAGNET

FIGURE 2

that the maximum field generated was reduced by approximately 40% when the magnets were interleaved. Finally, the design had one coil providing flux to three pole tips. This reduced the efficiency and hence the flux available at the gap.

Several approaches to improving the efficiency of the magnetic undulator were studied prior to constructing additional magnet structures. One way to increase the available flux is to reduce the gap between the pole tips. This option was not available due to the size of the electron beam (see Appendix A). Another way to increase the flux is to increase the total current around the baseplate. Increasing the cross-sectional area of the pole tips and increasing the period (and thus reducing the losses between adjacent pairs of poles) were two other proposals to reduce the losses experienced by Ellis.

The first change made was to remove the center set of pole tips and use these tips to double the pole piece and pole tip cross sections. The period was increased from 5.0 cm to 9.5 cm. These changes resulted in little increase in the field strength between the pole tips; however, the area over which the field was at a maximum was doubled. When the magnets were interleaved the losses were now approximately 10% compared to the same structures separated (Table 1). As the generation of PSER requires the interleaving of the magnets to form a periodic magnetic field, not only are large fields for isolated pole tips desireable, but it is

TABLE 1

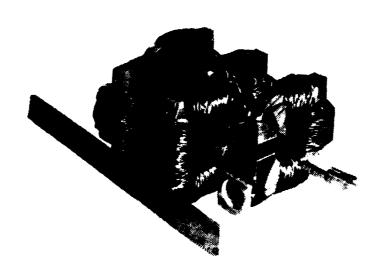
	•			Magnetic	Magnetic field (GAUSS) at	AUSS) at	
Configuration	# Turns of Wire	Period	6 amps	8 amps	8 amps 10 amps 12 amps	12 amps	14 amps
Ellis-modified	100	NA	250	375	575	625	800
Ellis-modified	150	NA	900	625	800	950	1100
Ellis-modified	150	9.0 cm	900	625	750	! !	
C-Magnet	300	NA	006	1100	1250	1350	1425
C-Magnet	300	9.0 cm	:	1 ! !	850	1050	1100
Permanent	NA	9.5 cm	1	1	1000	0	!!!

also necessary to minimize the losses when the pole tips are interleaved.

The next change made was to increase the number of turns of wire on the magnets from 100 to 150. This resulted in an increase in the peak field of just under 50% when the magnets were not interleaved. When the magnets were interleaved the losses were now about the same (10%) as with 100 turns.

The final analysis of the Ellis magnet and subsequent modifications made to it led to the following conclusions: A period of between 7.0 and 10.0 cm will reduce the losses due to interleaving to less than 20%. A minimum of 150 turns of wire and a coil current of 12 A will be necessary to generate the desired kilogauss field. The power requirements would be excessive unless each pole piece was wound separately or a high current/water cooled magnet winding was used.

The next iteration is depicted in Figure 3. The C-type magnet structure was chosen because it is the most efficient shape for generating high magnetic fields [Ref. 7]. Each C-magnet was wound with 300 turns of wire. The C-magnets proved excellent for generating magnetic fields of one kilogauss and higher. When an undulator of two and one half periods was constructed with a period of 9.0 cm, the fields were approximately 80% of the fields generated by the free standing C-magnets (Table 1). The power required to drive the five C- magnets was appreciable and scaled to a



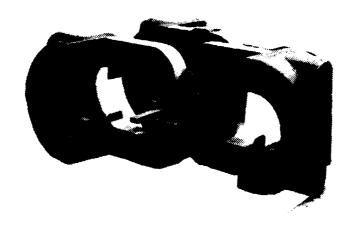
FIRST "C" MAGNET

FIGURE 3

requirement for more than 3500 watts of DC for an 11 period undulator. The C-magnets also required extensive machine shop work for fabrication, were difficult to wind with wire without shorting the windings, were hard to align and were time consuming in varying the period. The option to alter the gap between the pole tips was not available if needed.

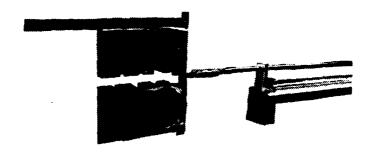
These factors led to a search for an alternative method of generating the desired fields. High strength permanent magnets were investigated (Figure 4). They appeared capable of generating the required field, but presented the problems of high cost and the inability to remotely switch the fields on and off, the latter feature being essential to compare the Cerenkov radiation and the PSER.

Another concept was presented by Jerry Graham [Ref. 8] for a comb-type magnet with two "combs" of alternately polarized magnets to be placed with the teeth facing each other. This configuration appeared to have significant potential and a prototype was built (Figure 5). The prototype comb magnet demonstrated its feasibility by generating fields of greater than one kilogauss with good heat dissipation characteristics. The power required scaled to 1800 watts for an 11 period undulator. Each pole piece was wound with 150 turns of magnet wire. Two complete periods were constructed and tested (Figures 6, 7 & 8). The design for the final undulator assembly was based upon the performance of this prototype.



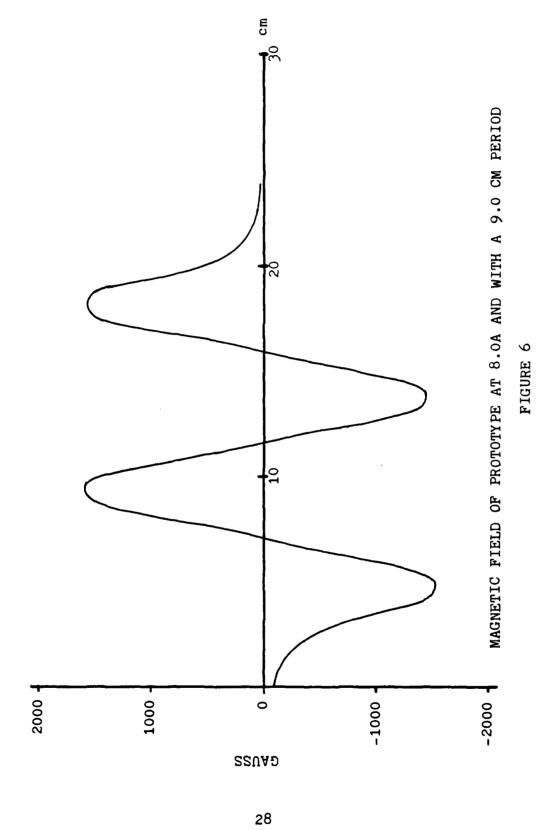
PERMANENT MAGNET

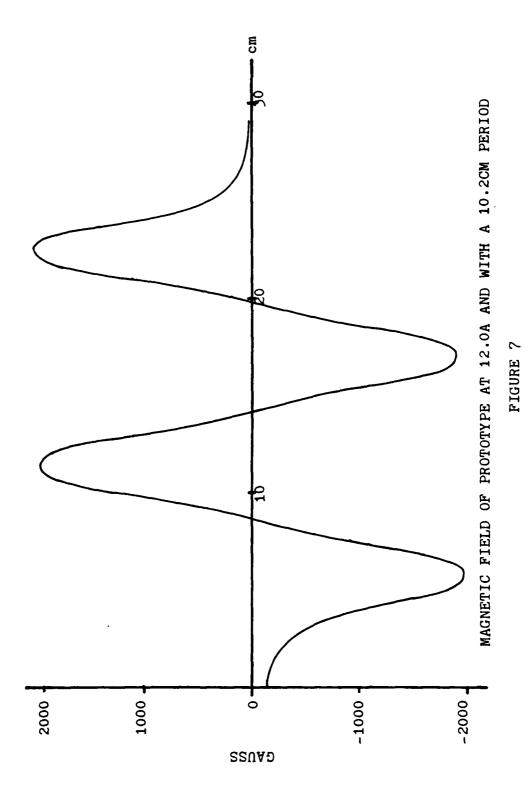
FIGURE 4

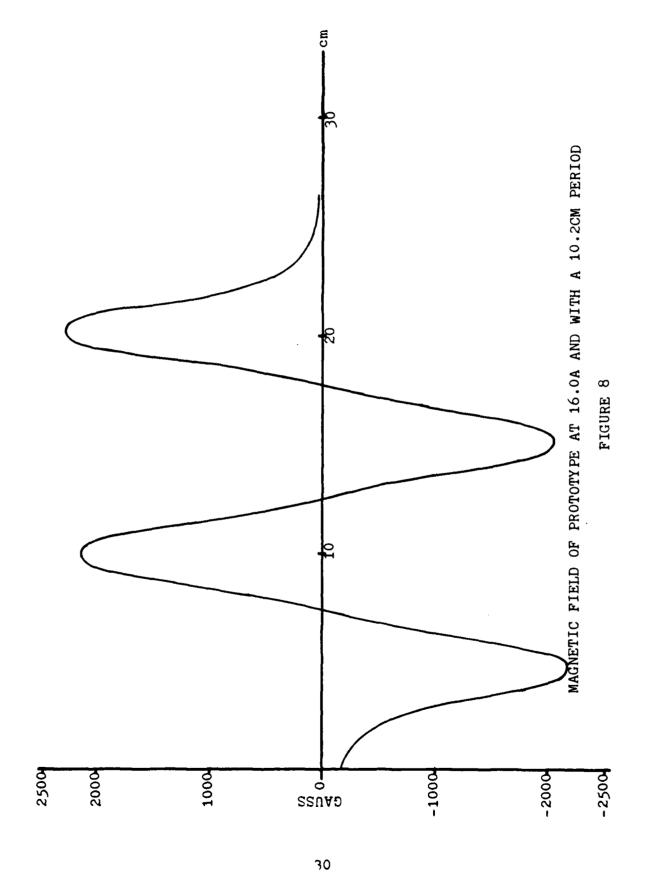


PROTOTYPE COMB MAGNET

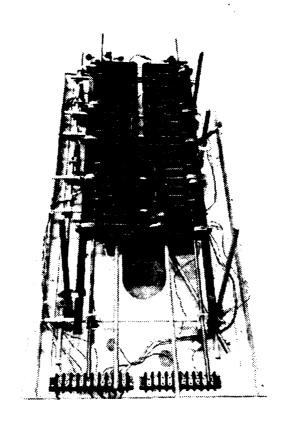
FIGURE 5





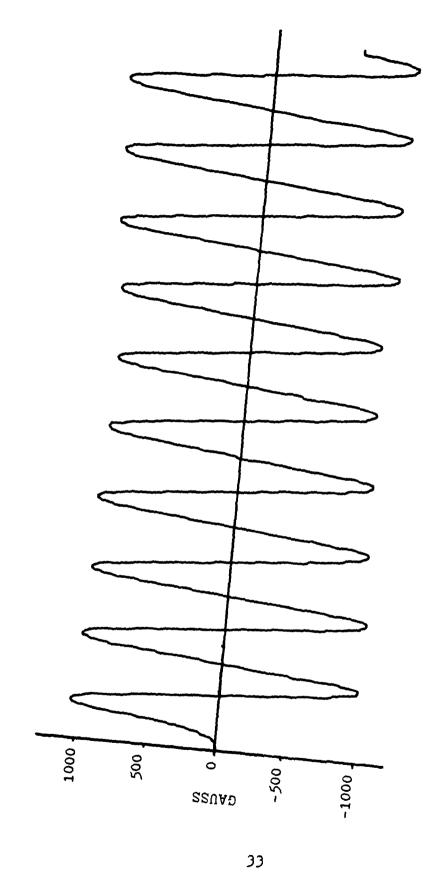


The final undulator (Figure 9) is noteworthy in that it required a minimum of machine shop work, was made from common materials (mild 1040 steel throughout) and provided a maximum amount of flexibility, allowing both variation of the period and the gap. Provisions for additional pole tips to spread the magnetic field in the vertical direction were To determine the optimum number of turns of magnet wire for each pole piece, 12 pole pieces were wound, four with 180 turns, four with 240 turns and four with 300 turns. A lathe was used to wind the pole pieces. The twelve test pole pieces were then run at high currents (10 to 15 A), both with and without a cooling fan, to determine to optimum number of turns of wire. Given the capabilities of the power supplies and the projected use of a mylar envelope to contain the helium, this limiting the ability to use a cooling fan, the pole tips with 180 turns performed the best and were chosen for the final undulator. Bench tests of the final undulator assembly showed that sustained periodic magnetic fields of 1600 gauss and pulsed fields of up to 2000 gauss could be generated. These were obtained with the magnets configured for a period of 9.0 cm. When the 3/4 in. bars at the bases of the pole pieces were removed these fields were reduced by approximately 10%. The magnetic fields generated by pairs of pole tips fluctuated less than five percent from the mean (Figures 10 & 11). With the additional pole tips in place the field intensity was reduced by approximately 1/3 and the field was spread in the



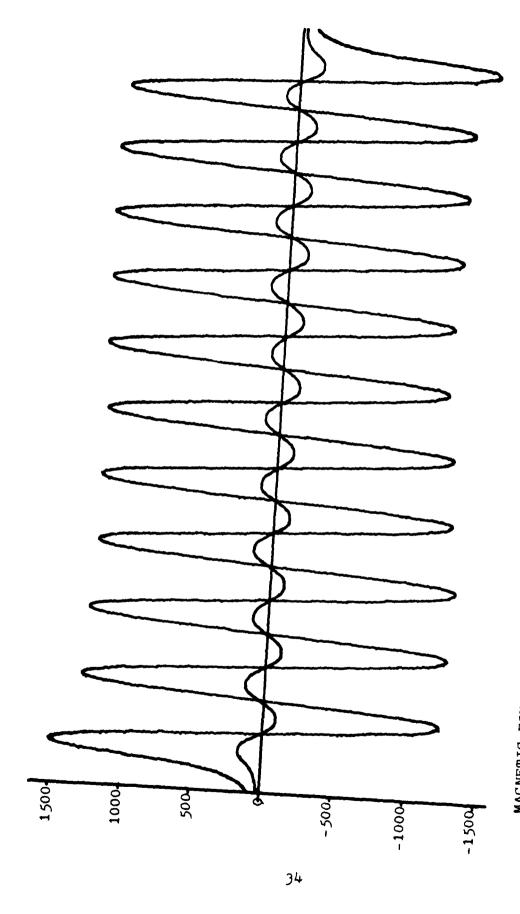
FINAL MAGNETIC UNDULATOR

FIGURE 9



MAGNETIC FIELD OF FINAL MAGNET AT 8.0A WITH A 9.0CM PERIOD

FIGURE 10



MAGNETIC FIELD OF FINAL MAGNET AT 10.0A WITH A 7.0CM PERIOD AND RESIDUAL MAGNETISM

FIGURE 11

vertical direction over an area approximately 50% larger than without the additional pole tips. The gaps between the pole tips could be adjusted to within \$1.0 mm of any desired gap, both with and without the additional pole tips in place. In the experiment the additional pole tips were not used, the higher magnetic fields being desired. The entire assembly of 11 periods could be powered by 1800 watts DC (120 V @ 15 A). For the final undulator configuration the period was set at 7.0 cm. This was done to minimize the amount of radiation blocked by the magnets and to produce the highest frequency PSER possible.

IV. EXPERIMENTAL PROCEDURE

In the initial configuration, the electron beam exited a five mil aluminum window, transversed a 20 cm layer of air, and entered the cavity of the magnetic undulator. The electron beam then passed through a diffuse reflector and was incident upon a secondary emission monitor. The radiation produced by the passage of the beam through the air was incident on the diffuse reflector and monitored by an RCA vidicon camera. The radiation was then observed with the undulator off, with a residual field of 100 gauss, and with the undulator at a value of 1500 gauss. No effects were discernible. The RCA camera has an automatic electronic light control which would suppress any intensity change. The diffuse reflector was replaced with an aluminum mirror to enhance the amount of light entering the camera. There were still no discernible effects.

A substantial problem was encountered with the spreading of the electron beam by the aluminum window and the air. The scattering mechanism is discussed in Appendix A, and the results are summarized in table 2. Note that by far the greatest scattering contributions are from the aluminum window and the air. Even the substitution of a one mil stainless steel would not reduce the scatter. The air was replaceable with different gases.

TABLE 2

Scatterer	Material	Mean Scatter Angle
exit window	5 mil aluminum	.008 radians
exit window	1 mil S. Steel	.008 radians
Air	110 cm	.007 radians
Helium	110 cm	.002 radians
Air	20 cm	.003 radians
Helium	80 cm	.001 radians
entrance window	1 mil al-mylar	.002 radians
exit window	1 mil mylar	.002 radians
entrance window	2 mil polystyrene	.001 radians

It is evident that the air adds a substantial amount to the beam spreading. Additionally, the air has a much larger angle of emission for Cerenkov radiation. This also is discussed in Appendix A, with the results summarized in table 3.

TABLE 3

Beam Energy	Medium	Cerenkov Angle
100 Mev	Air	.0298 radians
100 Mev	Helium	.0072 radians

It is this large Cerenkov angle that produces a very large shadow effect, i.e. the pole tips of the undulator clearly outlined in the image of the radiation cone. To reduce both the beam spread from air, and the angle of emission of Cerenkov radiation, a helium filled pipe was placed in the undulator cavity. The pipe was made of stainless steel, with a length of 80 cm, and radius of .9 cm.

Measurements in helium were also the ultimate goal since helium has a simple dielectric structure, and passage of ultraviolet light is better because the first resonance is higher than the strong resonances of air. The entrance window was made of one mil aluminized mylar. The entrance window served to block the Cerenkov radiation produced in the 20 cm of air. The exit window was made of one mil mylar.

The emitted radiation was again incident upon the plane mirror and observed with the camera. The radiation was observed with the residual field and with the undulator at 1500 gauss. There was no effect associated uniquely with the expected PSER effect. There was a problem of alignment, corrected later with a helium-neon laser. This alignment problem causeded unexpected patterns to be noticed. These patterns were probably due to internal reflections in the tube. In this regard, however, the tube did serve to confine all the radiation produced in a clear circular pattern.

In order to eliminate the pattern obstruction due to the pipe, the pipe was removed and replaced by a two mil polystyrene cover. This cover surrounded the entire undulator. To add a quantitative measure of intensity change, a silicon photocell was added to the camera. This camera and photocell arrangement is discussed in Appendix D. A spherical mirror was also added to increase the amount of light entering the camera. A flourescent screen was added to the back of the plane aluminum mirror to aid in the alignment of the beam, and to determine the size of the beam. The configuration is described in figure 20.

This arrangement produced some important results. The beam was still enlarged enough to produce a shadow effect, i.e. the pole tips of the undulator were clearly outlined on the flourescent screen. The radiation cone produced an even larger shadow effect.

As a test of the purity of the helium, the beam energy was reduced to 65 Mev. This is the threshold value for the production of Cerenkov radiation in helium (Appendix A). A distinct cone was noticeable. The energy was reduced down to 30 Mev, but the cone did not disappear. From this, it was deduced that there was a large quantity of air in the envelope. Air has a threshold at 22 Mev.

Data were taken at this configuration. Although an attempt was made to hold the beam current steady, it is not certain that this was done. There was also considerable noise from the photocell (Appendix D). Therefore the results are highly suspect. The results of the runs are listed in table 4 for a beam energy of 95 MeV, and in table 5 for a beam energy of 57 MeV.

	TABLE 4	(95 Mev)	
BEAM MONITOR (AMPS)	3 X 10 ⁻⁸	2 X 10 ⁻⁸	2 X 10 ⁻⁸
BASE LEVEL (VOLTS)	1.49	1.51	1.51
BEAM ONLY (VOLTS)	1.59	1.56	1.57
UNDULATOR (VOLTS)	1.65	1.61	1.61
PERCENTAGE CHANGE	60	100	67
	TABLE 5	(57 Mev)	
BEAM MONITOR (AMPS)	9 X 10 ⁻⁹	9 X 10 ⁻⁹	8 x 10 ⁻⁹
BASE LEVEL (VOLTS)	1.53	1.53	1.53
BEAM ONLY (VOLTS)	1.608	1.624	1.611
UNDULATOR (VOLTS)	1.608	1.619	1.621
PERCENTAGE CHANGE	0	- 5	12

To reduce the noise of the photocell, a new cable was installed. To measure the photocell voltage and the beam current simultaneuosly, a HP digital voltmeter was added to amplify the beam current of about 10⁻⁸ amps to a proportional signal of several volts. To reduce the beam spread, an extension pipe was added at the exit window, extending the exit window inside the helium envelope to the undulator cavity. This reduced the scattering due to 20 cm of air, and the beam was observed on the flourescent screen to produce no shadow. The radiation cone still produced a shadow. There was a slight change in the pattern of the cone with the undulator on. This is discussed in Chapter V. The data taken at 95 Mev are in table 6.

TABLE 6 (95 Mev)

	PHOTOCELL (VOLTS)	BEAM (VOLTS)
BASE LEVEL	•933	0
BEAM ONLY	1.224 1.227 1.235	4.488 4.456 4.504
UNDULATOR	1.146 1.142 1.154	4.398 4.439 4.539

Subtracting out the base level, and taking the average photocell voltage divided by the average beam voltage, the resulting intensity loss is 27%.

V. ANALYSIS

At the conclusion of the experimental portion of this project, many of the findings were preliminary. A variation of the intensity of the PSER with respect to the Cerenkov radiation was noted. With a mixture of helium and air, the PSER was approximately 1.5 times as intense as the Cerenkov radiation. With pure helium, a decrease of 10% intensity of PSER with respect to Cerenkov radiation was noted. Our theoretical analysis predicts an increase of intensity of 1.3 for PSER relative to the intensity of the Cerenkov radiation in helium. Using equation II-15

$$\frac{dW}{dz_m} = 1.4 \times 10^{-12}.$$

Using equation II-16 gives

$$\frac{dW}{dz}_{C} = 4.35 \times 10^{-12}$$
.

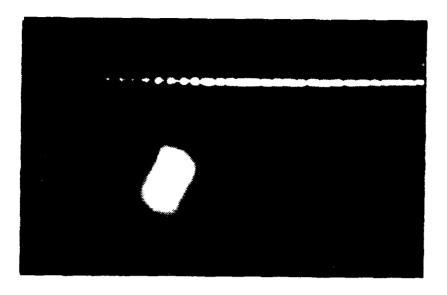
The ratio of these values is

$$\frac{dW_{T}}{dW_{C}} = 0.31.$$

Since the total PSER is the longitudinal component plus the transverse component, and since the longitudinal value is approximately equal the Cerenkov value, the total intensity of PSER relative to the Cerenkov is 1.31.

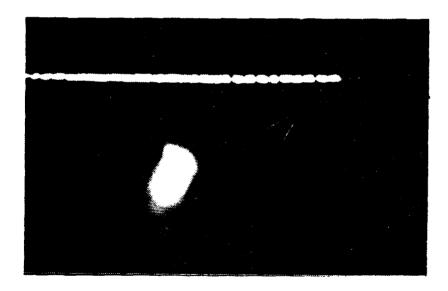
The radiation pattern generated by the PSER from the helium and air mixture was different from the Cerenkov radiation, the PSER pattern being longer from top to bottom and having a slight gap about 1/4 of the way from the top (Figures 12 & 13). With a helium environment, the changes were so small that they were virtually impossible to verify using the vidicon equipped television camera. Small fluctuations in the electron beam intensity caused similar changes in the pattern, effectively masking the effect of the pump field. For a helium environment the theoretical value for the Cerenkov angle is $\phi_{\rm c} = 0.5488^{\circ}$ and the theoretical value for the mach angle is $\phi_{\rm m} = 0.5428^{\circ}$. This small difference was not observable using the television camera.

The experimental arrangement used had several limitations. The exit window of the LINAC scattered the electron beam to the extent that the beam diameter was almost 2.0 cm at the far end of the undulator. This resulted in the PSER and Cerenkov radiation patterns being less distinct than desireable. The gap between the pole tips of the undulator could not be made greater than 2.0 cm without reducing the magnetic field below the desired field strength. As a result part of the radiation was blocked by the last few periods of the undulator. There does not appear to be an easy solution to this problem. The optical effects of the spherical mirror were never completely eliminated as a possible source of error (see Appendix D).



RADIATION PATTERN FOR CERENKOV RADIATION

FIGURE 12



RADIATION PATTERN FOR PSER RADIATION

FIGURE 13

One possible explanation of the differences in the PSER with a helium and air mixture compared to helium only, may be due to "wobbling." Wobbling, in this context, was coined to describe the effect caused by the transverse oscillatory motion of the electron causing a decrease in the longitudinal velocity. The latter decrease could cause the electrons to be subluminal or possibly decrease the amount of radiation slightly from those portions of the path which had the lower velocity. In the formulation of Schneider and Spitzer [Ref. 3], it is the longitudinal velocity which enters the equation for energy. Therefore, if the electron does wobble in and out of superluminal condition, the approximation that the longitudinal energy per unit path length is equal to the Cerenkov energy per unit path length may not be valid. In this case, an actual decrease in the observed intensity would be possible, and may explain the results of the experiment.

Schneider and Spitzer give the superluminal condition to be [Ref. 3] $\overline{\beta}_z^2 n^2 > 1$, where

$$\overline{\beta}_{2}^{2} = \beta^{2} - \frac{1}{2}(\omega_{1}/\gamma\omega_{0})^{2}. \qquad (V-1)$$

For the case of the pure helium, at 100 MeV, γ equals 195. For a magnetic field of 1500 gauss, ω_1 equals 2.63 x 10^{10} . For a spatial period of seven cm, ω_0 equals 2.69 x 10^{10} . Substitution into V-1 yields

$$\overline{\beta}_{z}^{2}n^{2} = 1.0000334$$
.

For 100 Mev electrons, the superluminal condition is met.

From equation V-1, the threshold condition for the electrons is

$$\gamma_{\text{threshold}}^2 = (\omega_1/\omega_0)^2 (\beta^2 - 1/n^2)^{-1}.$$
 (V-2)

This yields a threshold energy of 43.2 MeV. Future observations may be able to detect this threshold.

A method of observing the PSER without the use of the spherical mirror could eliminate one possible source of error. The use of more pure helium may also yield better results. The aluminum exit window of the LINAC could be replaced with a one mil mylar window, substantially reducing the beam spread. Future observations about the threshold frequencies may also prove useful.

APPENDIX A

Beam Spread

For an approximation of the scattering angle of a charged particle passing through a medium, Segrè gives the equation [Ref. 9]

$$\langle \theta^2 \rangle = \frac{E_s^2 L Z^2}{(PV)^2 L_{rad}}.$$
 (A-1)

 $\rm E_{\rm S}$ is equal to 21.2 MeV, PV is the energy of the particle, Z is the charge of the particle, $\rm L_{\rm rad}$ is the radiation length in $\rm g/cm^2$, and L is the scattering length which is equal to the thickness of the scatterer times the density. For a relativistic electron, the above expression reduces to

$$<\theta^2> = (.045) L/L_{rad}$$
 (A-2)

when the energy is 100 Mev.

The following radiation lengths are taken from Segrè with the exception of Mylar which is calculated based on its chemical composition:

MATERIAL	$\frac{L_{rad}}{(g/cm^2)}$	DENSITY (g/cm ³)
Aluminum	23.9	2.7
Helium	85.0	0.179×10^{-3}
Air	36.5	1.30×10^{-3}
Polystyrene	43.4	1.05
Mylar	40.1	1.39 .

The radius of the electron beam at any point along its axis is a function of its initial radius, $r_{\rm o}$, at the aluminum exit window, and any radius increments due to scatterers along the path. For a thin, relatively dense scatterer, the incremental radius at the target is

$$\langle \delta r \rangle = \langle \theta^2 \rangle^{\frac{1}{2}} D \tag{A-3}$$

where D is the distance from the scatterer to the target.

For a gaseous scatterer, the incremental radius is [Ref.10]

$$\langle \delta r \rangle = (\langle \theta^2 \rangle / 3)^{\frac{1}{2}} D.$$
 (A-4)

For several scatterers along the axis of the electron, the total incremental radius is

$$<\delta r_{\text{total}}^2> = <\delta r_1^2> + <\delta r_2^2> + \cdots <\delta r_n^2>$$
 (A-5)

where there are n scatterers. The total radius of the beam at the target then is

$$r_{\text{beam}} = r_0 + \langle \delta r_{\text{total}}^2 \rangle^{\frac{1}{2}}$$
 (A-5)

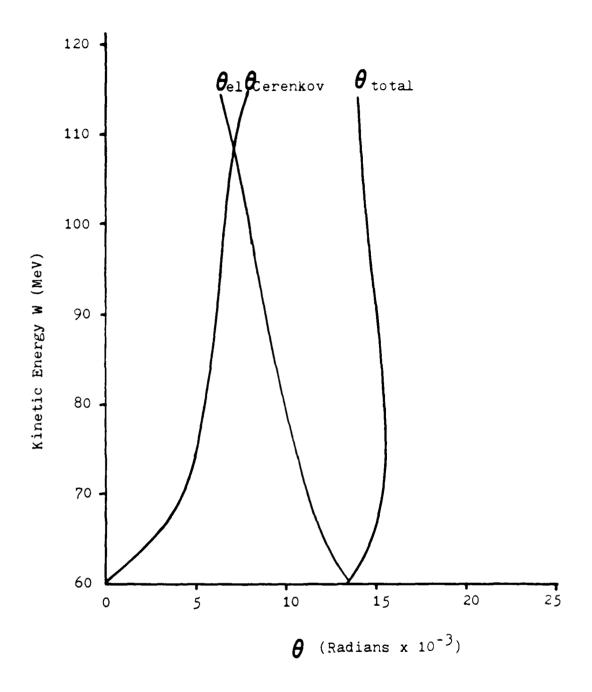
For the final experimental configuration, the estimated beam radius on the flourescent screen was one cm. Assuming an intial radius of 0.2 cm, equation A-5 gives a value for the radius of 1.1 cm.

For determination of the radius of the Mach cone, the Cerenkov or PSER angle is added to the angular deviation of the outermost electron from the electrons' longitudinal axis at the point where the initial radiation is produced. For helium, in the final configuration, the Cerenkov angle is .007 radians from an index of refraction equal to 1.000036

[Ref.11]. The initial radiation is produced at the exit window, so the angular deviation of the electron from its longitudinal path is due only to the aluminum window. This deviation is .008 radians, so the total deviation of the electron from its longitudinal path is .0015 radians. This results in a Mach cone of approximately two cm, which is close to the observed cone.

The threshold for the production of Cerenkov radiation is $\beta n > 1$. For helium, this is 60 Mev.

From equation II-20 for the Cerenkov angle, it is clear that as the energy of the electron increases, the Cerenkov angle also increases. From equation A-1, however, it can be seen that as the energy increases, the scattering angle decreases. Figure 14 is a graph of these two angles, and the resultant curve shows that there is little change in the total scattering angle with a change in energy.



GRAPH OF CERENKOV ANGLE vs. SCATTERING ANGLE OF EXIT WINDOW

FIGURE 14

APPENDIX B

PSER Thresholds

The kinematical analysis of a fast electron interacting with a static, periodic magnetic field gives the correct values for α_+ and α_- . This analysis is simpler than that of Schneider and Spitzer [Ref. 3], and is in agreement with their expressions for the thresholds.

The electron is traveling to the right with velocity $\boldsymbol{v}_{e}.$ Its position is given by

$$x_{\rho} = v_{\rho} t_{\rho} + x_{O} . \tag{B-1}$$

The static, periodic field is represented by

$$B = B_0 \cos(k_1 x). \tag{B-2}$$

The electron will move according to

$$\frac{dP_e}{dt} = F = qv_eB . (B-3)$$

The displacement is

$$y = A \cos (k_1 x_e + \phi).$$
 (B-4)

Then solving for \dot{P}_y and setting this equal to F gives

$$\dot{y} = -k_1 v_e \sin (k_1 x_e + \Phi)$$
 (B-5)

$$P_{v} = P_{x} (v_{v}/v_{x}) = -k_{1}A \sin(k_{1}x_{e} + \Phi)$$
 (B-6)

$$\dot{P}_{v} = -k_{1}v_{e}A \cos(k_{1}x_{e} + \Phi) = qv_{e}B_{0} \cos k_{1}x_{e}.$$
 (B-7)

This gives

$$A = -qB_0/k_1 , \qquad \Phi = 0 , \qquad (B-8)$$

and

$$\dot{y} = -k_1 v_e \sin(k_1 x_e). \tag{B-9}$$

The generated wave is

$$E' = E'_{0} \cos \left(\overline{k}_{2} \cdot \overline{r} - \omega_{2} t + \Phi'\right)$$
 (B-10)

and the force on the electrons is qE'. The electric field along the trajectory at the space-time position of the electron is given by

$$E' = E'_0 \cos \left(k_2 \cos \theta \ x_e - \omega_2 t_e + \Phi' \right) \tag{B-11}$$

or E'= E'_{0} cos [(
$$k_{2}$$
cos $\theta - \frac{\omega_{2}}{v_{e}}$) $x_{e} + \frac{\omega_{2}x_{0}}{v_{e}}$]. (B-12)

From equation B-9

$$v_y = -k_1 v_e A \cos(k_1 x_e + 90^\circ).$$
 (B-13)

The force acting on the electron must be in the opposite direction to the velocity of the electron if there is to be a net energy transfer to the radiation. Assuming the v_y is small compared to v_x , then equating the arguments of the cosine functions in equations B-12 and B-13 (and noting that $\cos \alpha$ is equal to $\cos(-\alpha)$ gives two cases. Case I:

$$\frac{\omega_2 x_0}{v_e} = 90^{\circ} \text{ and } k_1 = k_2 \cos\theta - \frac{\omega_2}{v_e} = k_2 (\cos\theta - 1/n\beta)$$

where

$$k_i = \omega_i / v_i$$
; then for $\theta = 0$

$$\omega_{+} = \omega_{0} \beta n \frac{\beta n - 1}{\beta^{2} n^{2} - 1}$$
 where $\omega_{0} = \frac{2\pi c}{n \lambda_{0}}$

Case II:

$$\frac{\omega_2 x_0}{v_e} = -90^\circ \text{ and } -k_1 = k_2 \cos\theta - \frac{\omega_2}{v_e} = k_2 (\cos\theta + 1/n\beta);$$
for $\theta = 180^\circ$

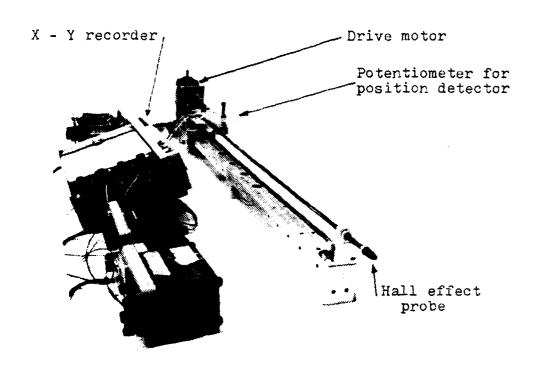
$$\omega_- = \omega_0 \beta n \frac{\beta n + 1}{\beta^2 n^2 - 1} .$$

These values are in agreement with Schneider and Spitzer. When further developed, they produce some results which are not in agreement with Schneider and Spitzer, such as the variation of α as a function of θ , as outlined in Ref. 3.

APPENDIX C

Traveling Magnetic Field Fluxmeter

After a brief attempt to use a laboratory type Hall Effect fluxmeter to measure the magnetic fields generated by the undulator, the need for a method of accurately measuring the magnetic fields was apparent. A traveling probe fluxmeter was designed and constructed (Figure 15). A Hall Effect element was mounted at the end of the probe. output was connected to the Y direction drive on an X - Y recorder. A drive wheel connected to a potentiometer was used to produce a position indicating output. This was fed to the X direction drive on the X - Y recorder. A large permanent magnet was calibrated using a laboratory rotating tip fluxmeter (accurate to 1.0%). This permanent magnet was determined to have a field of 665 gauss constant over a 2.0 cm by 2.0 cm area. It was used to calibrate the Hall Effect element on the traveling fluxmeter for all subsequent tests.



TRAVELING FLUXMETER

FIGURE 15

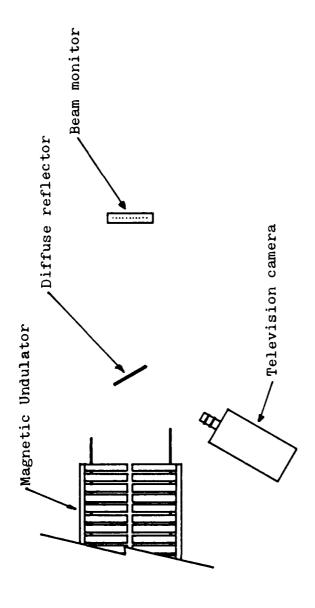
APPENDIX D

Optics

The radiation emitted by the electron beam - undulator field - helium interaction was of very low intensity, presenting problems in observation and measurement. Initially the radiation was observed using a plane diffuse reflector which was viewed with a vidicon equipped television camera. The camera output was viewed with a television monitor located in the LINAC control area. The radiation level was so low that the vidicon's threshold of sensitivity was approached (Figure 16). A plane mirror was next used to view the radiation pattern. This had the desired effect of increasing the amount of radiation reaching the vidicon, but had the disadvantage that the apparent intensity of the pattern was not constant, but varied across the image due to the diverging nature of the radiation (Figure 17). In order to quantize the change in intensity, a photoconductive photodiode detector was installed in the television camera (Figures 18 and 19). The PIN-6D photodiode was chosen and a mirror with approximately 85% reflectance was used. The sensitive area of the photodiode was determined by observing a constant intensity source and comparing the photodiode output to the position of the image on the television monitor. radiation is emitted at the characteristic angle throughout the undulator (See Chapter IV). In the final

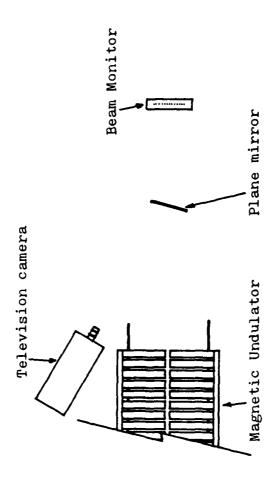
configuration the radiation was reflected by a plane mirror of highly polished aluminum placed approximately 10 cm from the end of the undulator. Aluminum was used as most glass mirrors become radioactive when exposed to high energy electrons. By having the mirror close to the undulator the amount of Cerenkov radiation generated by the electron beam passing through the air outside of the undulator was minimized. The radiation was projected on to a front silvered spherical mirror of 112 cm focal length (Figure 20). The spherical mirror serves as an imaging surface for the television camera and photodiode and concentrates the radiation on the lens of the camera. The camera is focused on the mirror and the image seen is the same as would be seen if a diffuse reflector was used as an imaging surface. As a large percentage of the incident radiation was focused to one small area, the proper alignment of the spherical mirror with respect to both the radiation and the camera was critical. Small vertical adjustments in the electron beam path required small corrections to the mirror alignment. As the source of the radiation varied in distance from the spherical mirror from 30 cm to 110 cm, the camera saw the apparent source of the radiation as behind the mirror. This is given by

$$S_i = \frac{S_o f}{S_o - f} .$$



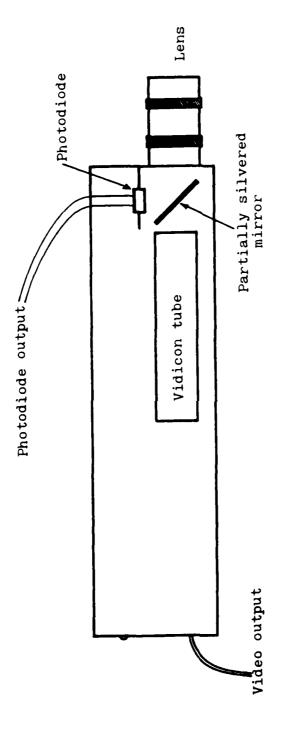
INITIAL OPTICAL CONFIGURATION

FIGURE 16



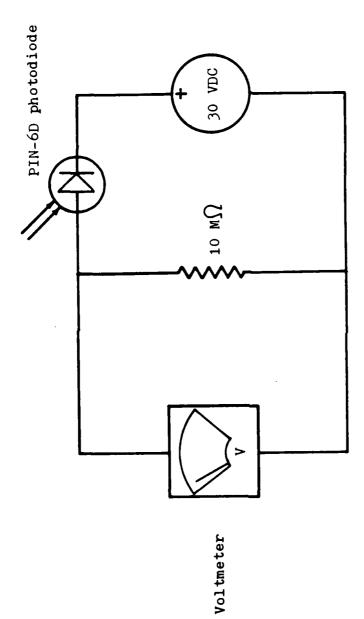
SECOND OPTICAL CONFIGURATION

FIGURE 17



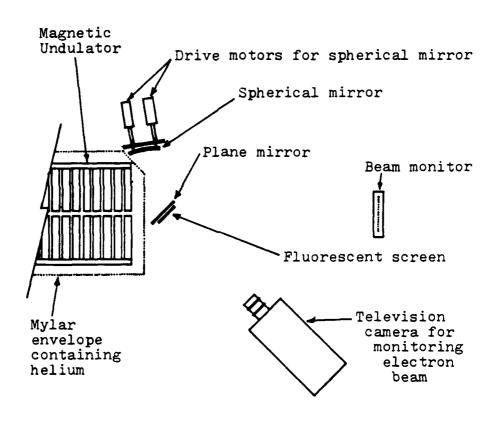
PHOTODIODE INSTALLED IN CAMERA

FIGURE 18



SCHEMATIC OF PHOTODIODE CIRCUIT

FIGURE 19



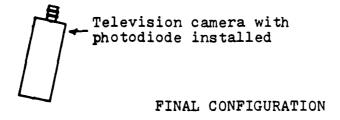


FIGURE 20

The resulting image distances relative to the mirror for the extreme ends of the undulator are

$$S_{i max} = -6160 cm$$

and
$$S_{i min} = -41 cm$$
.

This gave the apparent source distances varying between 225 cm and 6343 cm from the camera. The radiation was still diverging when it reached the camera and photocell, although the amount of divergence had been reduced by the spherical mirror. The varying source distance for the camera meant a larger percentage of the radiation from one part of the undulator was incident on the camera lens compared to the radiation from another part of the undulator. This could have help mask the differences between the PSER and Cerenkov radiation intensities.

The fluorescent screen on the back side of the plane aluminum mirror was used to determine if the electron beam was properly focused and centered in the undulator.

LIST OF REFERENCES

- 1. Richmyer, F. K., Kennard, E. H., and Cooper, J. N.,
 Introduction to Modern Physics, McGraw-Hill, 1969.
- Schneider, S., and Spitzer, R., "Stimulated Electromagnetic Shock Radiation," <u>Physics of Quantum Electronics</u>, v. 5, Addison-Wesley, 1978.
- 3. Schneider, S., and Spitzer, R., "Interaction of Electrons and Pump Fields at Superluminal Electron Velocities," paper presented at the ONR Workshop on Free Electron Generators, August 1979, Telluride, Colorado, and to be published in Physics of Quantum Electronics, v. 7, Addison-Wesley.
- 4. Ellis, R. B., Stimulated Emission by Relativistic Electrons Traversing a Periodic Magnetic Field, Master's Thesis, U.S. Naval Postgraduate School, Monterey, 1979.
- 5. Kroll, N. M., "Relativistic Synchrotron Radiation in a Medium and Its Implications for SESR," paper presented at the ONR Workshop on Free Electron Generators, August 1979, Telluride, Colorado, and to be published in Physics of Quantum Electronics, v. 7, Addison-Wesley.
- 6. Spitzer, R., Letter to Professor F. R. Buskirk, U.S. Naval Postgraduate School, 30 April 80, in regard to Ref. 3.
- 7. Edwards, A., "Magnet Design and Selection of Material," published in <u>Permanent Magnets and Magnetism</u>, ed. by Hadfield, D., John Wiley & Sons, Inc., London, 1962.
- 8. Graham, J., concept developed by, U.S. Naval Postgraduate School, Monterey.
- 9. Segre, E., <u>Nuclei and Particles</u>, W. A. Benjamin, Inc., New York, 1964.
- 10. Fermi, E., <u>Nuclear Physics</u>, compiled by Orear, J., and others, <u>University of Chicago</u> Press, Chicago, 1950.
- 11. Condon, E. U., and Odishaw, H., <u>Handbook of Physics</u>, McGraw-Hill Book Company, Inc., New York, 1958.

INITIAL DISTRIBUTION LIST

		No. Copies
1.	Defense Technical Information Center Cameron Station Alexandria, Virginia 22314	2
2.	Library, Code 0142 Naval Postgraduate School Monterey, California 93940	2
3.	Physics Library, Code 61 Department of Physics and Chemistry Naval Postgraduate School Monterey, California 93940	1
4.	Professor F.R. Buskirk, Code 61Bs Department of Physics and Chemistry Naval Postgraduate School Monterey, California 93940	5
5•	Colonel E. A. Saunders Head, Department of Physics U. S. Military Academy West Point, N.Y. 10996	1
6.	Commander U.S. Army Electronic Proving Ground Attn: S & I Branch Ft. Huachuca, Arizona 85613	1
7.	Cpt. William M. Decker IV U.S. Army Electronic Proving Ground Attn: S & I Branch Ft. Huachuca, Arizona 85613	1
8.	Cpt. Joseph P. Mackin Department of Physics U. S. Military Academy West Point, N.Y. 10996	1

